Am J Physiol Heart Circ Physiol 293: H3301–H3310, 2007.
First published September 14, 2007; doi:10.1152/ajpheart.00259.2007.

Hypertension-induced remodeling of cardiac excitation-contraction coupling in ventricular myocytes occurs prior to hypertrophy development

Ye Chen-Izu,[1] Ling Chen,[2] Tamás Bányász,[1,3] Stacey L. McCulle,[2] Byron Norton,[1] Steven M. Scharf,[2] Anuj Agarwal,[4] Abhijit Patwardhan,[4] Leighton T. Izu,[1] and C. William Balke[1,5]

[1]*Department of Internal Medicine, University of Kentucky College of Medicine, Lexington, Kentucky;* [2]*Department of Medicine, University of Maryland School of Medicine, Baltimore, Maryland;* [3]*Department of Physiology, University Medical School of Debrecen, Debrecen, Hungary; and* [4]*Center for Biomedical Engineering, University of Kentucky and* [5]*Department of Physiology, University of Kentucky College of Medicine, Lexington, Kentucky*

Submitted 2 March 2007; accepted in final form 11 September 2007

Chen-Izu Y, Chen L, Bányász T, McCulle SL, Norton B, Scharf SM, Agarwal A, Patwardhan A, Izu LT, Balke CW. Hypertension-induced remodeling of cardiac excitation-contraction coupling in ventricular myocytes occurs prior to hypertrophy development. *Am J Physiol Heart Circ Physiol* 293: H3301–H3310, 2007. First published September 14, 2007; doi:10.1152/ajpheart.00259.2007.—Hypertension is a major risk factor for developing cardiac hypertrophy and heart failure. Previous studies show that hypertrophied and failing hearts display alterations in excitation-contraction (E-C) coupling. However, it is unclear whether remodeling of the E-C coupling system occurs before or after heart disease development. We hypothesized that hypertension might cause changes in the E-C coupling system that, in turn, induce hypertrophy. Here we tested this hypothesis by utilizing the progressive development of hypertensive heart disease in the spontaneously hypertensive rat (SHR) to identify a window period when SHR had just developed hypertension but had not yet developed hypertrophy. We found the following major changes in cardiac E-C coupling during this window period. *1*) Using echocardiography and hemodynamics measurements, we found a decrease of left ventricular ejection fraction and cardiac output after the onset of hypertension. *2*) Studies in isolated ventricular myocytes showed that myocardial contraction was also enhanced at the same time. *3*) The action potential became prolonged. *4*) The E-C coupling gain was increased. *5*) The systolic Ca^{2+} transient was augmented. These data show that profound changes in E-C coupling already occur at the onset of hypertension and precede hypertrophy development. Prolonged action potential and increased E-C coupling gain synergistically increase the Ca^{2+} transient. Functionally, augmented Ca^{2+} transient causes enhancement of myocardial contraction that can partially compensate for the greater workload to maintain cardiac output. The increased Ca^{2+} signaling cascade as a molecular mechanism linking hypertension to cardiac hypertrophy development is also discussed.

heart failure; action potential; L-type Ca^{2+} channel; ryanodine receptor

SYSTEMIC HYPERTENSION is a major risk factor for cardiac hypertrophy and heart failure. The severe impact of hypertensive heart disease (HHD) is underscored by the fact that ~30% of the US adult population have hypertension (17) and 60% of these develop cardiac hypertrophy (13, 36). However, the cellular and molecular mechanisms linking hypertension to heart diseases remain unclear. Extensive evidence has demonstrated that cardiac hypertrophy is associated with remodeling of the excitation-contraction (E-C) coupling system and enhanced myocardial contraction (11, 22, 33), and heart failure is marked by diminished contractility (2, 3, 6, 18). An important yet unanswered question is whether changes in E-C coupling are directly linked to hypertension or are merely markers of later-stage hypertrophy. We hypothesized that hypertension might directly cause remodeling of the cardiac E-C coupling system.

Previous studies using hearts that had already developed significant hypertrophy or heart failure were confounded by difficulties in separating the causal mechanism of disease from markers of advanced pathological conditions. To test our hypothesis, here we exploited the progressive development of HHD through distinct disease stages in the spontaneously hypertensive rat (SHR) (12, 32). With the SHR model, we identified a "window" period when the animals had just developed hypertension but before the development of cardiac hypertrophy. Our studies reveal a direct link between hypertension and profound changes in cardiac E-C coupling at both the whole heart and cellular levels. An interesting new finding is that the systolic function in vivo was depressed by hypertension before the development of "compensated hypertrophy," while at the same time, myocardial contraction was enhanced. Importantly, we found that the enhancement of myocardial contraction is caused by concerted changes in cellular E-C coupling, suggesting an immediate link between the onset of hypertension and an upregulation of the Ca^{2+} signaling that is expected to induce hypertrophy and heart failure on prolonged exposure to systemic hypertension.

MATERIALS AND METHODS

Animals and blood pressure measurement. Male SHR and normotensive Wistar-Kyoto rats (WKY) were purchased from Harlan (Indianapolis, IN) at the age of 4–5 wk. Blood pressure (BP) was monitored weekly in nonanesthetized rats with the standard noninvasive tail cuff method (IITC, model 29-SSP). Animal handling and all procedures were performed strictly in accordance with National Institutes of Health (NIH) guidelines and the Institutional Animal Care and Use Committee protocols approved by the University of Kentucky and by the University of Maryland.

Echocardiographic measures of cardiac function. The animals were anesthetized with 1.5% isoflurane supplemented with O_2. Echocardiography was performed with a SonoHeart Elite echocardiograph (SonoSite, Bothell, WA) equipped with a C11/7-4 11-mm broadband curved array transducer. Two-dimensional guided M-mode images of

Address for reprint requests and other correspondence: Y. Chen-Izu, Dept. of Internal Medicine, Univ. of Kentucky Coll. of Medicine, BBSRB, Rm. B255, 741 S. Limestone St., Lexington, KY 40536-0509 (e-mail: yechen-izu@uky.edu).

The costs of publication of this article were defrayed in part by the payment of page charges. The article must therefore be hereby marked "*advertisement*" in accordance with 18 U.S.C. Section 1734 solely to indicate this fact.

the left ventricle (LV) were taken with the parasternal short-axis view at the level of the papillary muscles. M-mode measurements included LV anterior-posterior cavitary dimension at end systole (LVDs) and end diastole (LVDd). Fractional shortening (FS) of the LV was calculated as [(LVDd − LVDs)/LVDd] × 100. LV ejection fraction was calculated as [(LVVd − LVVs)/LVVd] × 100, where LVVd is LV end-diastolic volume and LVVs is LV end-systolic volume. LVVd and LVVs were calculated as LVVd = [7/(2.4 + LVDd)] × $LVDd^3$ and LVVs = [7 × $LVDs^3$/(2.4 + LVDs)] (35).

Cardiac catheterization. Animals were anesthetized with 2.5% isoflurane supplemented with O_2, intubated, and ventilated via a rodent ventilator (Harvard Instruments, Holliston, MA). Rectal temperature was monitored and maintained at 37.5–38°C. A 3-Fr Mikro-tipped pressure transducer (SPR-249A, Millar Instruments, Houston, TX) was inserted into the aortic arch for measurement of BP and then advanced into the LV for measurement of LV pressure. A 1.4-F Mikro-tipped pressure transducer (SPR-671, Millar Instruments) was inserted into the vena cava for measurement of central venous pressure. Data were collected with the MP100 system (BioPac Systems, Goleta, CA). After a 30-min stabilization period, both transducers were removed and replaced with a thermistor-tipped catheter (3F, Edwards Lifesciences, Irvine, CA) into the aorta and a PE-25 catheter into the right atrium. Cardiac output was measured in triplicate with a cardiac output computer (Vigilance, Edward Lifesciences), by injecting 0.3 ml of iced saline into the right atrium and sampling the temperature from the aorta.

Cell isolation. The rats were anesthetized with Nembutal (100 mg/kg ip). After testing for the suppression of reflexes, the hearts were explanted via midline thoracotomy. A standard enzymatic technique was used to isolate the ventricle myocytes. Briefly, the heart was mounted on a Langendorff system and perfused with a modified Tyrode solution containing (in mmol/l) 135 NaCl, 4 KCl, 1.0 $MgSO_4$, 0.34 NaH_2PO_4, 15 glucose, 10 HEPES, and 10 taurine, pH 7.25 (adjusted with NaOH), for ~4 min; the perfusion solution was prewarmed to 37°C and bubbled with 100% O_2. Collagenase B (~1 mg/ml, F. Hoffmann-La Roche), protease type XIV (~0.1 mg/ml),

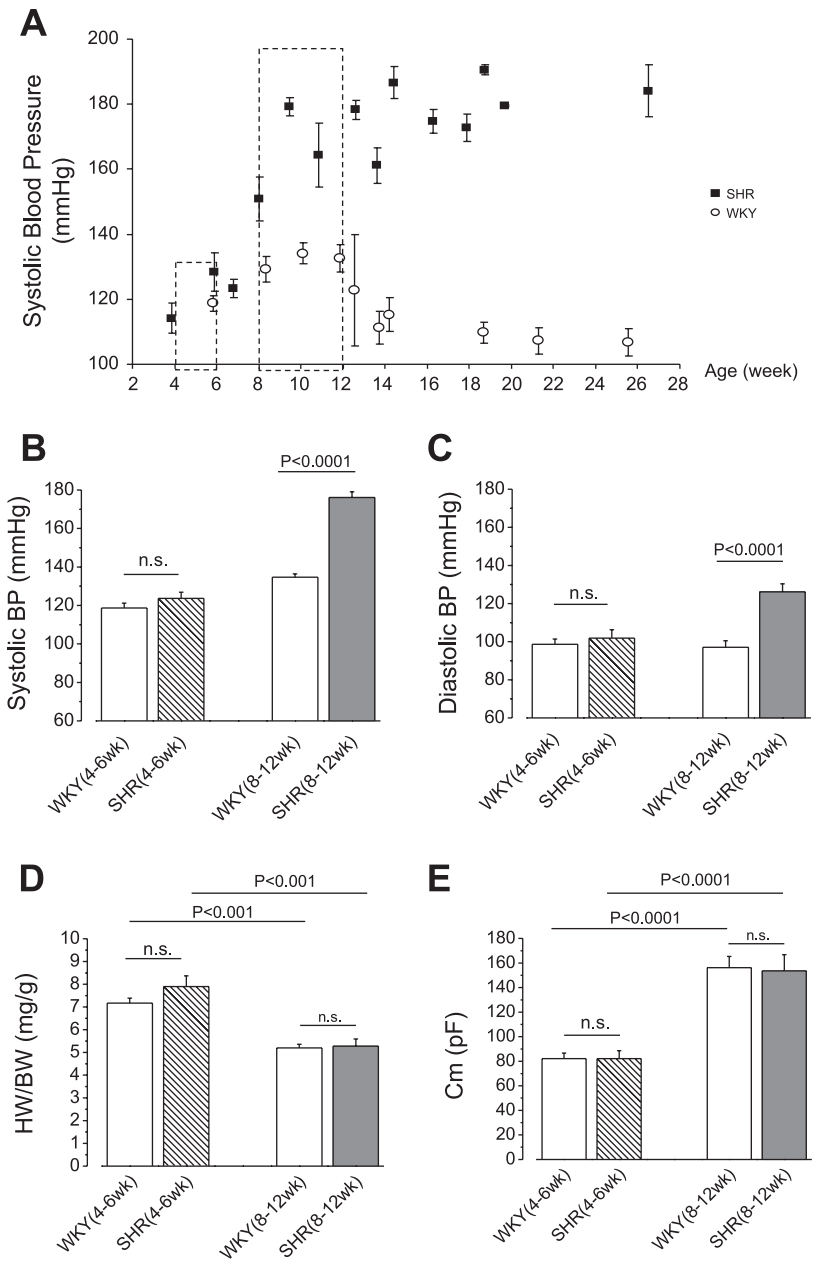

Fig. 1. Blood pressure (BP) was measured by standard tail-cuff method. *A*: time course for hypertension development in the spontaneously hypertensive rat (SHR) compared with the Wistar-Kyoto rat (WKY). Shown are mean ± SE values obtained from SHR and WKY groups (6–24 individual animals in each group). *B*: average systolic BP in 4- to 6-wk-old WKY [WKY(4–6 wk); $n = 21$] and SHR [SHR(4–6 wk); $n = 36$] and in 8- to 12-wk-old WKY [WKY(8–12 wk)] and SHR [SHR(8–12 wk)]. *C*: average diastolic BP in WKY(4–6 wk) ($n = 52$) and SHR(4–6 wk) ($n = 56$) and in WKY(8–12 wk) and SHR(8–12 wk). Cardiac hypertrophy was measured in (from *left* to *right*) WKY(4–6 wk), SHR(4–6 wk), WKY(8–12 wk), and SHR(8–12 wk) with 2 indexes: the wet heart weight-to-body weight ratio (HW/BW, from *left* to *right* $n = 5$, 7, 11, and 11 animals; *D*) and the whole cell membrane capacitance of ventricular myocytes (C_m, from *left* to *right* $n = 18$, 16, 13, and 12 cells; *E*). As the animals grew older, HW/BW decreased owing to a larger increase in BW than HW, while C_m of cells increased in correspondence to growth of the cell size. However, there was no significant difference between SHR and age-matched WKY in either HW/BW or C_m, demonstrating an absence of cardiac hypertrophy at the tissue and cell levels. n.s., Not significant.

Table 1. *Echocardiographic parameters and body weight of SHR at onset of hypertension in comparison to age-matched WKY*

Echocardiographic Parameters	WKY 8 wk	SHR 8 wk	WKY 12 wk	SHR 12 wk
Body wt, g	208.5±29.5	195.5±17.2	281.7±19.1	297.7±22.1*
Heart rate, beats/min	349.3±15.0	368.0±39.3	328.3±16.0	355.7±22.5
LV dimension-diastolic, mm	6.38±0.13	6.49±0.21	6.72±0.15	7.15±0.08†
LV dimension-systolic, mm	2.57±0.10	2.81±0.32	2.93±0.28	3.53±0.18†
LV fractional shortening, %	59.8±1.2	56.8±3.7	56.3±3.9	50.6±2.6*
LV ejection fraction, %	91.8±2.5	90.7±2.3	90.3±2.4	86.3±2.1*
LV posterior wall thickness-diastolic, mm	0.94±0.17	0.95±0.04	1.00±0.13	1.23±0.61*
LV posterior wall thickness-systolic, mm	2.30±0.32	2.17±0.08	2.28±0.22	2.43±0.15*
LV posterior wall fractional thickening, %	59.1±3.2	56.1±2.2	56.2±3.4	49.0±4.0*

Values are means ± SD; $n = 6$ for each group. SHR, spontaneously hypertensive rat; WKY, Wistar-Kyoto rat; LV, left ventricle. Student's *t*-test: *$P < 0.05$, †$P < 0.001$.

0.1% BSA, and 20 μM Ca^{2+} were then added into the perfusion solution, and the heart was digested for ~15 min. The ventricular tissue was cut down and minced with tissue scissors; the remaining tissue was further incubated in the enzyme solution at 37°C and minced again to collect isolated ventricular myocytes. The cells were stored in Tyrode solution containing 1 mM Ca^{2+} at room temperature and used within 10 h after isolation.

Chemicals and reagents were purchased from Sigma-Aldrich unless otherwise specified.

Ventricular myocyte contraction measurement. Load-free contraction of isolated ventricular myocytes was measured with the IonOptix system (IonOptix), which records the sarcomere pattern to calculate the changes in the sarcomere spacing with a fast Fourier transform algorithm. The cells were field stimulated (voltage pulse of 4 ms and 5–20 V across the chamber) at 1-Hz frequency and room temperature (22–23°C).

Sharp electrode measurement of action potentials. Action potential was measured from LV tissue with the sharp electrode technique. The tissue was continuously superfused in the bath solution containing (in mmol/l) 120 NaCl, 4 KCl, 1 $MgCl_2$, 1 $CaCl_2$, 25 $NaHCO_3$, 10 HEPES, and 10 glucose, pH 7.3 (adjusted with NaOH). The tissue was paced at 500-ms cycle length with 3-ms biphasic stimuli delivered through a bipolar platinum-iridium electrode. After at least 1-h preconditioning at room temperature to reach steady state, the recordings were made with glass microelectrodes filled with 3 M KCl. Data were analog filtered at 20 KHz and sampled at a rate of 10,000 samples/s.

Whole cell voltage clamp. The whole cell voltage-clamp technique was used to simultaneously record L-type Ca^{2+} current [$I_{Ca(L)}$] and intracellular Ca^{2+} concentration ([Ca^{2+}]). Briefly, cells were continuously superfused with bath solution containing (in mmol/l) 135 NaCl, 4 CsCl, 0.33 $NaHPO_4$, 1 $MgSO_4$, 10 HEPES, 10 glucose, and 1 $CaCl_2$, pH 7.3 (adjusted with NaOH). Voltage-clamp protocols were generated and currents recorded with an Axopatch 200B amplifier and a DigiData 1200B analog-to digital (A/D) converter (Axon Instruments) under computer control. The following voltage-clamp protocol was used for recording $I_{Ca(L)}$ and $[Ca^{2+}]_i$. The holding potential was set to −80 mV. First, a depolarizing step to −40 mV of 800-ms duration was used to inactivate Na^+ channels. Second, a test pulse of 200-ms duration was used to record the current-voltage (*I-V*) relationship of $I_{Ca(L)}$. Third, the cell was repolarized to the holding potential. The interval between pulses was set to 5 s to allow sufficient time for the Ca^{2+} transient to return to the resting level. No preconditioning was used for *I-V* measurement. For sarcoplasmic reticulum (SR) load measurement, the cell was preconditioned by repetitive depolarizing pulse from −80 mV to 0 mV to reach steady state before the caffeine depletion experiment. Series resistance compensation and supercharging were used to reduce the voltage offset and to speed up the capacitive transient. Currents were filtered at 2 kHz with an analog 4-pole Bessel filter and digitized at 5 kHz. To record $I_{Ca(L)}$, we used a pipette solution containing (in mmol/l) 130 glutamic acid, 130 CsOH, 20 CsCl, 10 HEPES, and 0.33 $MgCl_2$, pH 7.2 (adjusted with CsOH).

Epifluorescence microscopy. $[Ca^{2+}]_i$ was measured with indo-1 K salt (Molecular Probes/Invitrogen), which was added into the pipette solution (113 μM) and diffused into the cell. An inverted microscope equipped with a ×100 oil-immersion fluorescence objective (Nikon) was used, and a UV lamp (Photon Technology International) delivered an excitation beam of 365 nm to the cell on the microscope stage. Fluorescence emission was recorded at 405-nm and 485-nm wavelengths with photomultiplier tubes (Thorn EMI). The signals were analog filtered at 0.5 KHz, digitized with a DigiData 1200B A/D converter (Axon Instruments), and recorded simultaneously with $I_{Ca(L)}$. The ratio between indo-1 signals at 405 (F_{405}) and 485 (F_{485}) nm (R) was then calculated after subtracting the background fluorescence F^b_{405} and F^b_{485} (obtained before breaking into the whole cell configuration). The R values in 0 Ca^{2+} (R_{min}) and in saturating Ca^{2+} (R_{max}) were obtained by a previously described method (34). The time course of the fluorescence ratio [R(*t*)] was best fitted to the function

$$R(t) = \frac{F_{405} - F^b_{405}}{F_{485} - F^b_{485}} = a_0[1 - e^{-a_1(t - a_2)}] \times e^{-a_3(t-a_4)} \times H(t - a_2) + a_5 \quad (1)$$

where H(*t*) = 1 for $t \geq 0$, H(*t*) = 0 for $t < 0$, a_i ($i = 1...5$) are descriptional parameters that are used to fit R curve to exponential functions, and F^b denotes background fluorescence. $[Ca^{2+}]_i$ was calculated by substituting R from *Eq. 1* into the following equation (20)

Table 2. *Changes in cardiac performance at onset of hypertension in SHR*

Hemodynamic Parameters	WKY 12 wk	SHR 12 wk
Heart rate, beats/min	333.3±31.7	344.6±41.1
Systolic blood pressure, mmHg	102.7±7.9	178.3±22.7†
Mean arterial pressure, mmHg	85.3±9.2	139.3±18.0†
Diastolic blood pressure, mmHg	73.8±9.7	120.4±16.2†
Central venous pressure, mmHg	2.63±1.49	1.43±2.74
LV end-diastolic pressure, mmHg	10.2±2.5	9.2±1.7
Systemic vascular resistance, mmHg·ml^{-1}·min	1.44±0.26	2.94±0.61†
Cardiac output/body wt, ml·min^{-1}·kg^{-1}	206.7±19.3	159.7±17.4†
Stroke volume/body wt, ml/kg	0.62±0.02	0.47±0.03†
+dP/d*t*, mmHg/s	4,242.7±534.2	5,582.2±889.5†
−dP/d*t*, mmHg/s	−3,886.0±560.4	−6,163.4±972.0†

Values are means ± SD; $n = 10$. dP/d*t*, rate of change of pressure with time. Student's *t*-test: †$P < 0.001$.

$$[Ca^{2+}]_i = \beta \cdot k_D \frac{R - R_{min}}{R_{max} - R} \quad (2)$$

where β is an instrument-dependent scaling factor, which can be obtained from fitting the calibration curve. The maximum rate of rise of $[Ca^{2+}]_i$, $d[Ca^{2+}]_i/dt_{max}$, was used as an index of the maximal SR release flux, $J_{rel(max)}$ (34) (23). The E-C coupling gain was calculated as the ratio $J_{rel(max)}/I_{Ca(L)(peak)}$.

Statistics. Numerical values are presented as means ± SD in text and as means ± SE in figures unless otherwise noted. Unpaired Student's *t*-test with equal variance and two tails was used to evaluate the difference in the mean values, and the difference was deemed significant if $P < 0.05$. Two-way ANOVA test was used to compare between SHR and WKY (difference between strains) across the entire voltage range (difference between values at different voltages); Bonferroni posttest was used to evaluate the strain difference at each test voltage.

RESULTS

Onset of hypertension in SHR. To study the effect of hypertension without the confounding effects of cardiac hypertrophy, we identified a period at early phase of HHD when SHR had just developed hypertension but had not yet developed hypertrophy. BP measurements (Fig. 1*A*) showed that SHR were prehypertensive during their first 4–6 wk of life (systolic BP < 130 mmHg) and then rapidly developed hypertension between 8 and 12 wk of age. The average values of systolic (Fig. 1*B*) and diastolic (Fig. 1*C*) BP in 4- to 6-wk-old prehypertensive SHR were 124 ± 26 and 102 ± 27 mmHg ($n = 36$), respectively, similar to those in age-matched WKY (systolic BP 119 ± 11 mmHg and diastolic BP 99 ± 13, $n = 21$; *t*-test, $P = 0.6$ and 0.5). During the onset of hypertension between 8 and 12 wk of age, SHR developed high systolic and diastolic BP of 176 ± 22 and 126 ± 37 mmHg ($n = 52$), respectively, significantly higher than those in age-matched WKY (systolic BP 135 ± 17 mmHg and diastolic BP 97 ± 25, $n = 56$; *t*-test, $P = 8.1e{-}27$ and $4.8e{-}06$). After the onset of systolic and diastolic hypertension, SHR maintained essential hypertension throughout the development of cardiac hypertrophy and heart failure in 1.5–2 yr of life span (9).

Changes in cardiac performance at onset of hypertension. To study the changes in cardiac function at the onset of hypertension, echocardiography was performed in the SHR at 8 and 12 wk of age, which mark the start and the end of the window period for the onset of hypertension. As shown in Table 1, there was no significant difference in echocardiographic parameters between SHR and WKY at 8 wk of age. However, at 12 wk of age SHR displayed ~10% decrease in LV FS and 4.4% decrease in LV ejection fraction, demonstrating the effects of increased workload under hypertension. SHR also had larger LVDd and LV posterior wall thickness, which could be attributed to *1*) a faster growth of SHR than WKY (body wt 297.7 ± 22.1 vs. 281.7 ± 19.1 mg; *t*-test, $P < 0.05$) and *2*) possible hypertrophy or hyperplasia. The question of hypertrophy is addressed in *Window period at onset of hypertension before cardiac hypertrophy development* below.

We further examined hemodynamics in 12-wk-old hypertensive SHR compared with age-matched normotensive WKY, using catheter-based methods. As shown in Table 2, SHR displayed markedly elevated systolic and diastolic BP, and systemic vascular resistance was significantly increased by ~100%. Cardiac output and stroke volume were reduced by ~25%. Although the rate of change of pressure with time (dP/d*t*) was increased in SHR, after normalizing to the P value,

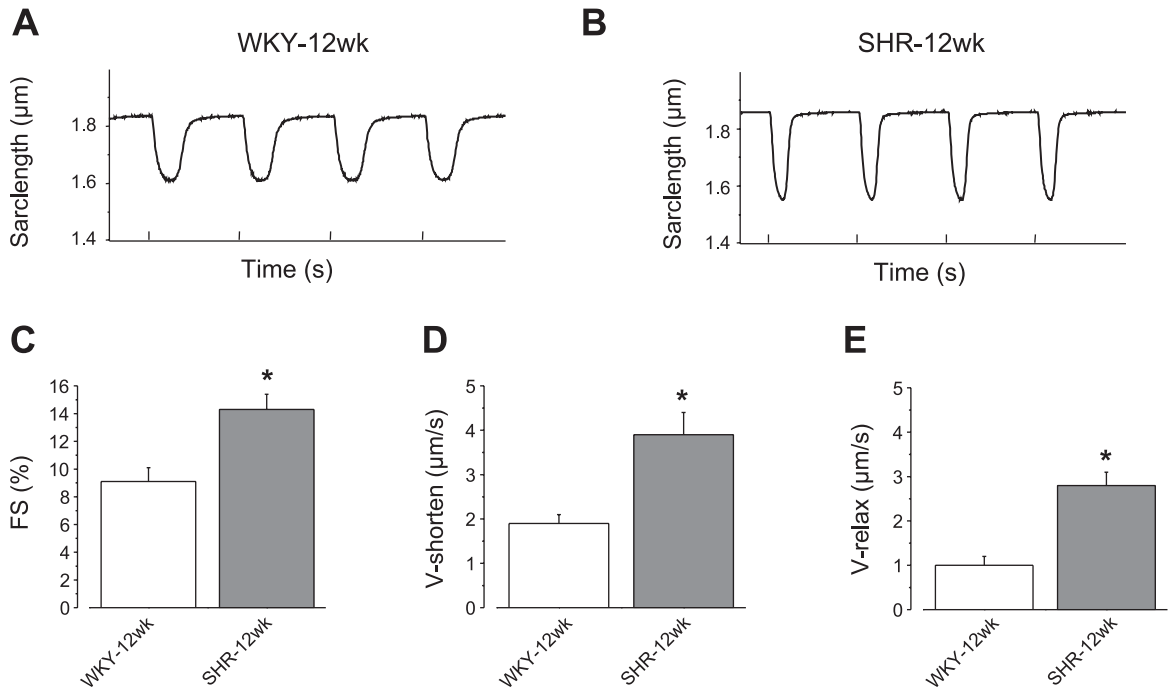

Fig. 2. *A* and *B*: load-free contraction of isolated ventricular myocytes was measured with the IonOptix system by tracking changes in sarcomere length. *C*: fractional shortening (FS), the ratio between the amplitude of cell contraction and the diastolic length, was larger in SHR than in WKY. *D*: velocity of contraction ($V_{shorten}$; μm/s per sarcomere), obtained by fitting the rising phase of the contraction curve with a single exponential function, was higher in SHR than in WKY. *E*: velocity of relaxation (V_{relax}; μm/s per sarcomere), obtained by fitting the declining phase with a single exponential function, was higher in SHR than in WKY. *$P < 0.05$, Student's *t*-test.

the average (dP/dt)/P values were 31 s^{-1} in SHR and 41 s^{-1} in WKY, indicating a decreased cardiac function consistent with decreased cardiac output and stroke volume. Thus the onset of hypertension is associated with a moderate depression in the cardiac pump function due to increased systemic vascular resistance.

Window period at onset of hypertension before cardiac hypertrophy development. We examined cardiac hypertrophy with two indexes, *1*) the wet heart weight-to-body weight ratio (HW/BW), which measures hypertrophy and hyperplasia at the tissue level, and *2*) the whole cell membrane capacitance in isolated ventricular myocytes, which most accurately measures hypertrophy at the cellular level (15). Figure 1, *D* and *E*, show that at 4–6 wk of age SHR and WKY had similar HW/BW (7.9 ± 1.1 mg/g in SHR vs. 7.2 ± 0.6 mg/g in WKY; *t*-test, $P = 0.16$) and similar whole cell membrane capacitance (82.2 ± 24.8 pF in SHR vs. 82.2 ± 18.4 pF in WKY; $P = 1.0$). In both SHR and WKY, as the animals grew older, HW/BW decreased, owing to a larger gain in BW than in HW, and cell membrane capacitance increased because of normal growth of the cell size. Nevertheless, compared with age-matched WKY, 8- to 12-wk-old SHR continued to display similar values in HW/BW (5.3 ± 1.0 mg/g in SHR vs. 5.2 ± 0.5 mg/g in WKY; $P = 0.83$) and in cell membrane capacitance (153.6 ± 43.8 pF in SHR vs. 156.2 ± 31.8 pF in WKY; $P = 0.87$), demonstrating a lack of discernible hypertrophy at the tissue and cell levels.

These data establish two distinct stages in HHD development in SHR: at 4–6 wk of age SHR are prehypertensive, and at 8–12 wk of age SHR become hypertensive but have not yet developed hypertrophy. Subsequent to this period, cardiac hypertrophy was found to develop progressively in SHR between 3 and 18 mo of age, and heart failure typically occurs between 18 and 24 mo of age as reported in previous publications from our group (9, 33) and others (14, 16).

Enhanced myocardial contractility at onset of hypertension. To study changes in cellular E-C coupling, we used isolated ventricular myocytes, which are removed from changes in BP or neuronal and hormonal influences in vivo. Figure 2 shows the measurements of the load-free cell contraction under field stimulation. Compared with age-matched WKY, the cells from 12-wk-old hypertensive SHR displayed significant increases in fractional shortening (14.3 ± 3.6% in SHR vs. 9.1 ± 3.4% in WKY; $P = 0.02$), velocity of shortening (−3.9 ± 1.6 vs. −1.9 ± 0.8 μm/s per sarcomere; $P = 0.02$), and velocity of relaxation (2.8 ± 1.2 vs. 1.0 ± 0.7 μm/s per sarcomere; $P = 0.01$). The diastolic sarcomere length was largely the same in the cells from SHR and WKY (1.82 ± 0.05 μm vs. 1.80 ± 0.02 μm; $P = 0.5$), indicating unchanged diastolic Ca^{2+} concentration. In comparison, 6-wk-old prehypertensive SHR had fractional shortening similar to that of age-matched WKY (9.4 ± 4.5% vs. 10.9 ± 4.3%, $n = 12$; $P = 0.5$).

Prolonged action potentials at onset of hypertension. Enhanced myocardial contraction could be influenced by two major factors: the action potential and the E-C coupling gain. We measured action potentials in LV tissue of 12-wk old SHR and WKY. Figure 3 shows that action potentials had significantly longer durations in SHR than in WKY. The action potential duration from the peak to 50% decay (APD_{50}), for example, was 39.8 ± 18.9 ms in SHR ($n = 4$ animals) versus 10.0 ± 2.7 ms in WKY ($n = 3$ animals; *t*-test, $P = 0.03$).

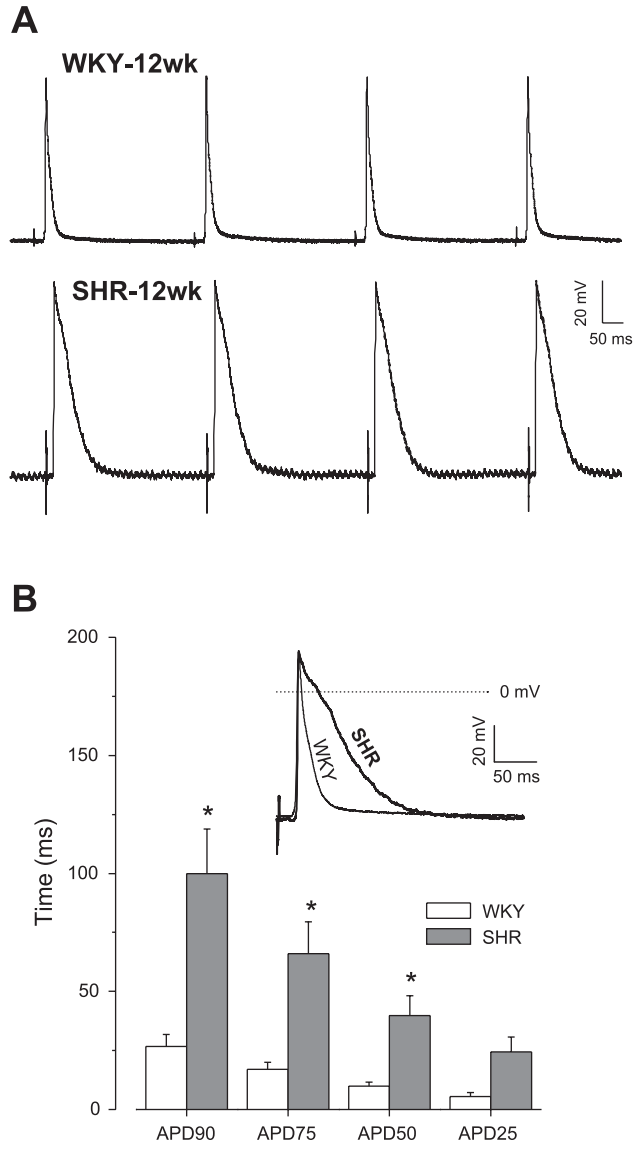

Fig. 3. Action potentials were recorded from left ventricular (LV) tissue. *A*: sample traces of action potentials from 12-wk-old WKY and SHR. *B*: action potential durations (APDs) were measured from the peak to 25% (APD_{25}), 50% (APD_{50}), 75% (APD_{75}), and 90% (APD_{90}) decay, which demonstrate significantly longer APD in SHR ($n = 4$ animals) than in WKY ($n = 3$ animals; $^*P < 0.05$, *t*-test) at APD_{50}, APD_{75}, and APD_{90}.

Prolonged action potential should allow more Ca^{2+} entry through L-type Ca^{2+} channels during excitation, boosting the trigger signal for E-C coupling.

$I_{Ca(L)}$ under voltage-clamp conditions. E-C coupling in ventricular myocytes was studied by simultaneously measuring $[Ca^{2+}]_i$ and $I_{Ca(L)}$ under whole cell voltage-clamp conditions. To investigate hypertension-related changes in cardiac E-C coupling, we used SHR at two distinctive stages: prehypertensive SHR between 4 and 6 wk of age [SHR(4–6 wk)] and hypertensive SHR between 8 and 12 wk of age [SHR(8–12 wk)]. Age-matched WKY groups [WKY(4–6 wk) and WKY(8–12 wk)] were used to separate age-related changes from disease-related changes.

We first examine $I_{Ca(L)}$ under voltage-clamp conditions. Figure 4, *A* and *B*, show representative $I_{Ca(L)}$ recordings from

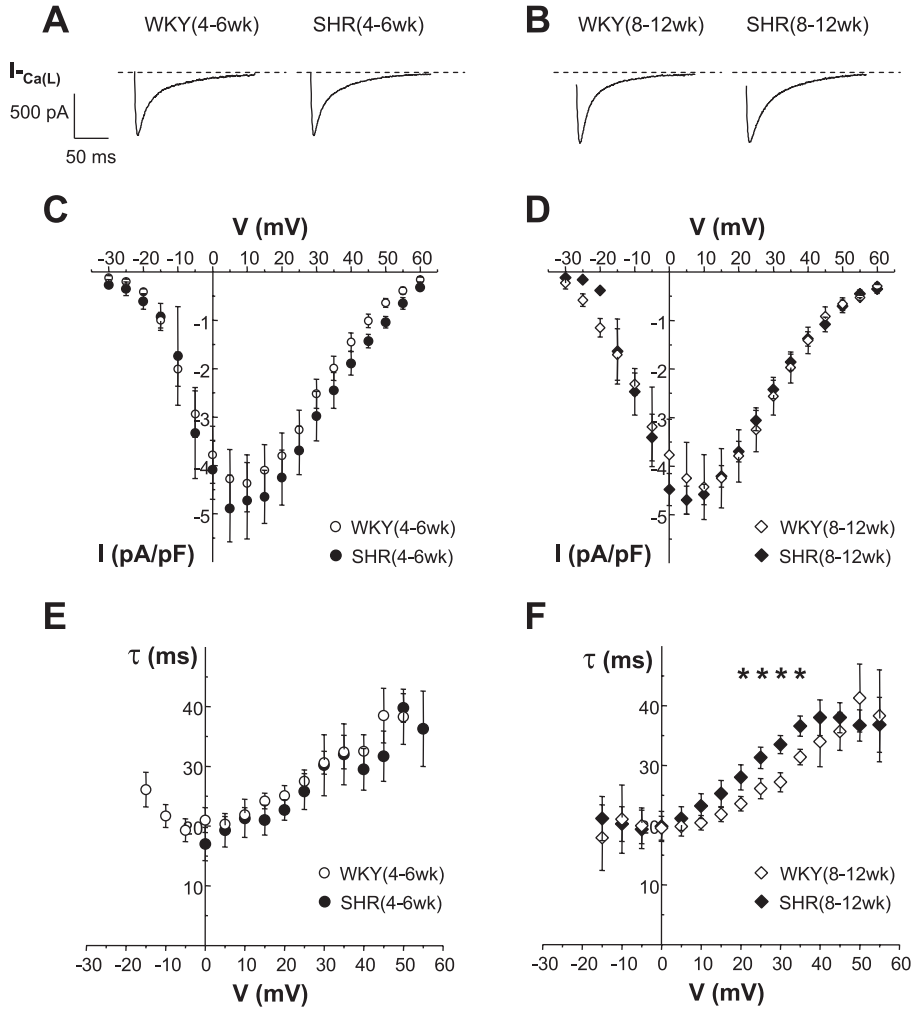

Fig. 4. The voltage (*V*)-clamp protocol consists of the following steps: the holding potential was set to −80 mV; the membrane potential was first depolarized to −40 mV for a duration of 900 ms to inactivate Na^+ channels; step pulses of 5-mV increments were then used to depolarize the membrane potential from −35 mV to +60 mV to measure L-type Ca^{2+} current [$I_{Ca(L)}$]. Sample traces of $I_{Ca(L)}$ during the depolarization pulse to +5 mV are shown (*A* and *B*). The peak current-voltage (*I-V*) relationship showed no significant difference between the strains in SHR(4–6 wk) vs. WKY(4–6 wk) (*C*) or in SHR(8–12) vs. WKY(8–12) (*D*). The inactivation rate of $I_{Ca(L)}$ (τ) was calculated by fitting the declining phase of $I_{Ca(L)}$ to a single exponential function. There was no significant difference in the inactivation rate between SHR(4–6 wk) and WKY(4–6 wk) (*t*-test, $P > 0.05$; *E*). SHR(8–12 wk) displayed slower τ than WKY(8–12 wk) in the voltage range between 20 and 35 mV according to Student's *t*-test (*$P < 0.05$; *F*). However, when 2-way ANOVA test with Bonferroni posttest is used to evaluate the statistical difference between SHR(8–12 wk) and WKY(8–12 wk) across the entire voltage range, Bonferroni posttest shows $P > 0.05$ for the difference in τ values.

WKY and SHR at prehypertensive (4–6 wk) and hypertensive (8–12 wk) stages. Figure 4, *C* and *D*, show the peak *I-V* relationship; there was no significant difference in all cell groups across the entire voltage range. For example, the peak $I_{Ca(L)}$ at 5 mV was −4.28 ± 1.72, −4.89 ± 1.39, −4.25 ± 1.95, and −4.70 ± 0.72 pA/pF for WKY(4–6 wk), SHR(4–6 wk), WKY(8–12 wk), and SHR(8–12 wk), respectively. The inactivation rate of $I_{Ca(L)}$ (τ) was largely the same between SHR(4–6 wk) and WKY(4–6 wk) (Fig. 4*E*). However, SHR(8–12 wk) displayed a slightly slower τ than WKY(8–12 wk) in the voltage range between 20 and 35 mV ($P < 0.05$) (Fig. 4*F*). There was no age-related change between WKY(4–6 wk) and WKY(8–12 wk) in either peak current density or τ.

$[Ca^{2+}]_i$ transient and SR Ca^{2+} release flux under voltage-clamp conditions. We next examine the $[Ca^{2+}]_i$ transient triggered by $I_{Ca(L)}$ (Fig. 5). SHR(4–6 wk) had a $[Ca^{2+}]_i$ transient similar to that of WKY(4–6 wk), with peak $[Ca^{2+}]_i$ of 0.76 ± 0.64 and 0.76 ± 0.58 μM, respectively (Fig. 5*C*). However, SHR(8–12 wk) displayed significantly higher peak $[Ca^{2+}]_i$ transient than WKY(8–12 wk) across a large voltage range between −10 and +30 mV (peak $[Ca^{2+}]_i$ at 10 mV: 3.64 ± 1.23 μM and 0.95 ± 0.57 μM; $P = 0.04$) (Fig. 5*D*). There was no detectable difference in the resting level $[Ca^{2+}]_i$ between SHR(8–12 wk) and WKY(8–12 wk) as indicated by indo-1 fluorescence ratio (0.68 ± 0.16 vs. 0.65 ± 0.17). Again, no age-related change in $[Ca^{2+}]_i$ was present between WKY(4–6 wk) and WKY(8–12 wk).

To isolate SR Ca^{2+} release from the other factors that also contribute to $[Ca^{2+}]_i$ such as Ca^{2+} sequestration and Na^+/Ca^{2+} exchange, we calculated the SR Ca^{2+} release flux (J_{rel}) at the initial moment of the $[Ca^{2+}]_i$ transient curve (see MATERIALS AND METHODS). At this initial moment, $[Ca^{2+}]_i$ was mainly set by the SR Ca^{2+} release, since the Ca^{2+} sequestration and Na^+/Ca^{2+} exchange processes had not yet come into play. Hence, J_{rel} gives us a measure of the SR Ca^{2+} release flux in response to the Ca^{2+} trigger $I_{Ca(L)}$. Figure 5*E* shows that SHR(4–6 wk) had J_{rel} similar to WKY(4–6 wk) across the entire voltage range. Importantly, SHR(8–12 wk) showed larger J_{rel} than WKY(8–12 wk) (Fig. 5*F*).

Increased E-C coupling gain at onset of hypertension. Knowing the trigger signal and the SR Ca^{2+} release flux, we can now calculate the E-C coupling gain by taking the ratio between J_{rel} and peak $I_{Ca(L)}$, gain = J_{rel}/peak $I_{Ca(L)}$. Figure 6 shows the E-C coupling gain in relationship to transmembrane voltage. While SHR(4–6 wk) had gain similar to WKY(4–6 wk) across the entire voltage range, SHR(8–12 wk) had significantly larger gain than WKY(8–12 wk) (2-way ANOVA test, $P < 0.0001$ for difference between strains). Therefore, at the onset of hypertension, SHR displayed higher E-C coupling

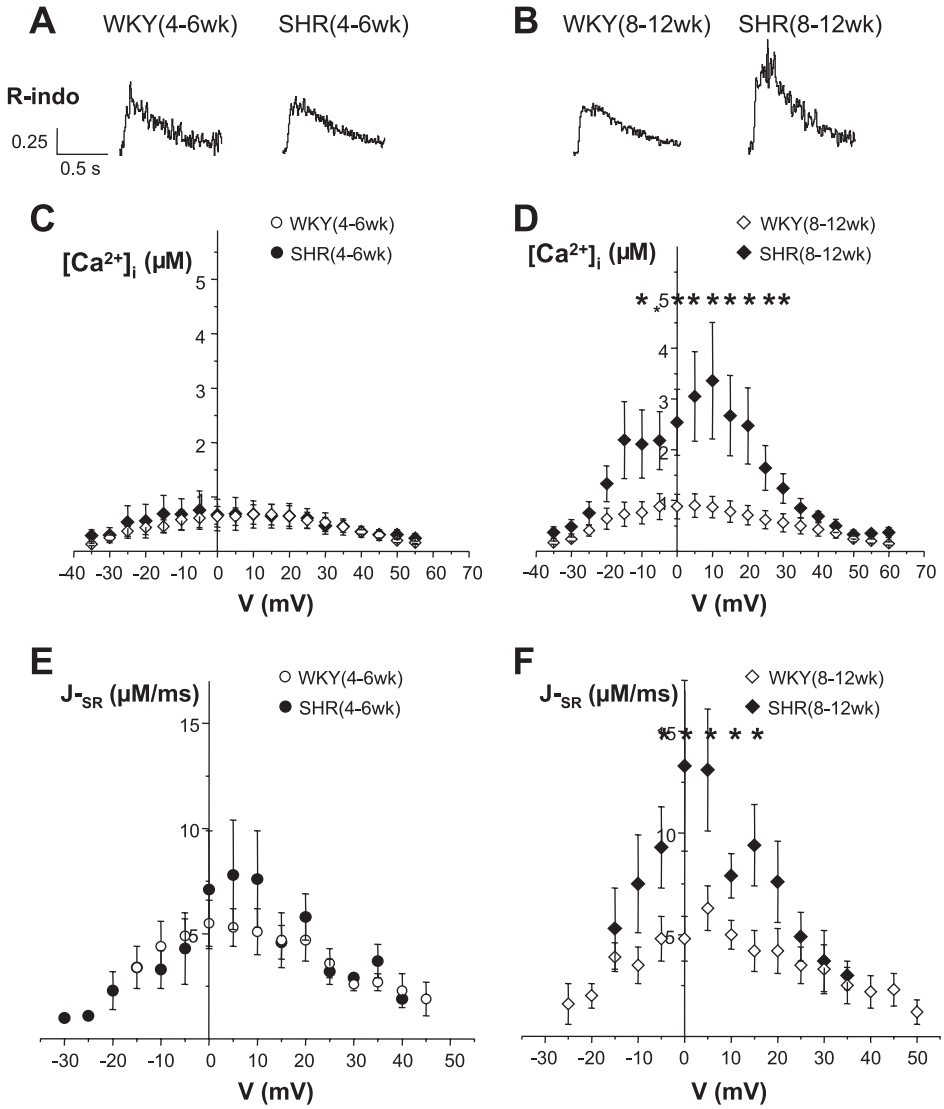

Fig. 5. Intracellular Ca^{2+} concentration ($[Ca^{2+}]_i$) transient triggered by $I_{Ca(L)}$ under voltage-clamp conditions as in Fig. 4 was measured with indo-1 fluorescence ratio [R_{indo} = fluorescence at 405 nm (F_{405})/fluorescence at 485 nm (F_{485})]. Sample traces of R_{indo} triggered by depolarizing the membrane potential to +5 mV are shown in *A* and *B*. There was no difference between SHR(4–6 wk) and WKY(4–6 wk) in their peak $[Ca^{2+}]_i$-voltage relationship (2-way ANOVA test, $P > 0.05$ for strain difference; *C*). However, SHR(8–12 wk) had significantly higher $[Ca^{2+}]_i$ than WKY(8–12 wk) (2-way ANOVA test, $P < 0.0001$ for strain difference, Bonferroni posttest $P < 0.05$ at $V = 5$ and 10 mV; $^*P < 0.05$, Student's *t*-test; *D*). Maximum sarcoplasmic reticulum Ca^{2+} release flux (J_{SR}) was calculated with a dynamic reaction scheme as described in MATERIALS AND METHODS. No significant difference was seen in J_{SR} between SHR(4–6 wk) and WKY(4–6 wk) (2-way ANOVA test, $P > 0.05$ for strain difference; *E*). SHR(8–12 wk) displayed higher J_{SR} than WKY(8–12 wk) (2-way ANOVA test, $P < 0.0001$ for strain difference, Bonferroni posttest $P < 0.05$ at $V = 5$ and 10 mV; $^*P < 0.05$, Student's *t*-test; *F*). There was no age-related difference between WKY(4–6 wk) and WKY(8–12 wk) in either $[Ca^{2+}]_i$ or J_{SR}.

gain. This increased gain might be caused by changes in the SR Ca^{2+} load or in the ryanodine receptor (RyR) activity.

Maintained SR Ca^{2+} load. As a key determinant of the E-C coupling gain, the SR Ca^{2+} load was examined by using caffeine (20 mM) to rapidly deplete the SR Ca^{2+} stores, while simultaneously measuring the $[Ca^{2+}]_i$ transient and the Na^+/Ca^{2+} exchange current (I_{NCX}) (Fig. 7). The total amount of SR Ca^{2+} release during the caffeine application (20 s) was calculated from the integral of I_{NCX} using a 3 Na^+/1 Ca^{2+} stoichiometry. Thus calculated, the total amount of SR Ca^{2+} load normalized to cell membrane capacitance for WKY(4–6 wk), SHR(4–6 wk), WKY(8–12 wk), and SHR(8–12 wk) was

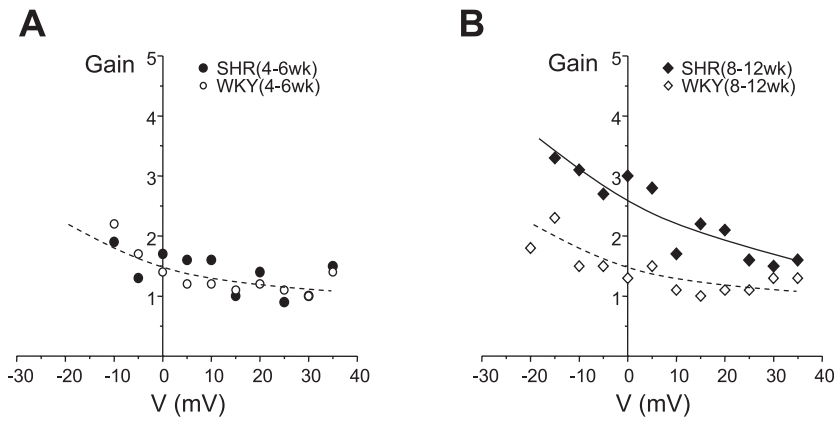

Fig. 6. Excitation-contraction (E-C) coupling gain was calculated as gain = J_{SR}/peak $I_{Ca(L)}$. No significant difference in gain was seen between SHR(4–6 wk) and WKY(4–6 wk) (2-way ANOVA, $P > 0.05$ for strain difference; *A*). However, SHR(8–12 wk) had higher E-C coupling gain than WKY(8–12 wk) across the voltage range (2-way ANOVA test, $P < 0.0001$ for strain difference; *B*).

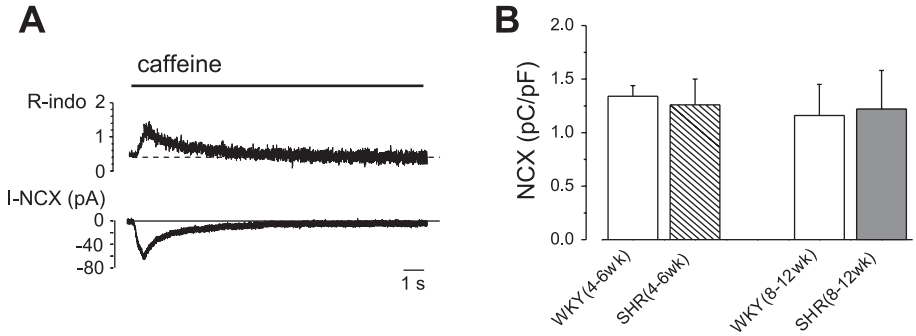

Fig. 7. SR Ca^{2+} load was measured with rapid application of caffeine (20 mM). *A*: sample traces of R_{indo} and Na^+/Ca^{2+} exchange current (I_{NCX}) recorded during caffeine application. The membrane potential was held at −80 mV throughout. The SR Ca^{2+} load was assessed by the total amount of Ca^{2+} excluded from the cell by NCX. To compare the SR load in different cells, the total NCX values are normalized to the cell sizes and have a unit of pC/pF. *B*: net charge movement through NCX (means ± SE): WKY(4–6 wk) (n = 6), SHR(4–6 wk) (n = 3), WKY(8–12 wk) (n = 5), and SHR(8–12 wk) (n = 4). No significant difference in NCX values was seen among all four cell groups, indicating no difference in the SR Ca^{2+} load.

1.34 ± 0.22, 1.26 ± 0.42, 1.16 ± 0.58 and 1.22 ± 0.72 pC/pF, respectively. There was no significant difference in the SR Ca^{2+} load among all cell groups.

DISCUSSION

We hypothesized that the onset of hypertension might cause immediate remodeling of the Ca^{2+} signaling system that alters whole heart function and induces cardiac hypertrophy. To test this hypothesis, we identified a window period in SHR when the animals had just developed hypertension but not yet developed hypertrophy. Thus changes in SHR observed during this period precede hypertrophy and can be attributed to the effects of hypertension.

First, we found that both systolic and diastolic BP increased rapidly in SHR between 8 and 12 wk of age (Fig. 1). During the same period the SHR heart had not yet developed detectable hypertrophy, although hypertrophy would later develop progressively in SHR between 3 and 18 mo of age (9, 14, 16, 33). Second, we found that the onset of hypertension in 12-wk-old SHR is associated with a decrease in cardiac output and stroke volume, demonstrating a depression of cardiac function under increased systemic vascular resistance (Table 2). This depression of cardiac function demonstrates an interesting contrast to the restored cardiac function after development of "compensated hypertrophy" at a later stage of HHD (4, 33). Third, dP/dt was increased in 12-wk-old SHR hearts, which could be explained by increased myocardial contractility or simply by increased P values. After normalization, (dP/dt)/P values show an average of 31 s^{-1} in SHR and 41 s^{-1} in WKY, again indicating depressed cardiac function. To further investigate possible changes in myocardial contraction, we used isolated ventricular myocytes, which allowed us to examine the changes at the cellular level separated from the BP change or neuronal/hormonal influences that affect whole heart function.

One major finding is that the ventricular myocyte from 12-wk-old SHR has enhanced contraction under field stimulation (Fig. 2). To investigate the cause for enhanced cell contraction, we examined the following important determinants of E-C coupling and found changes in SHR at the onset of hypertension compared with prehypertensive SHR or age-matched WKY controls. First, action potential measurements in LV tissue showed that SHR had markedly prolonged APD (Fig. 3), which should increase the Ca^{2+} entry through L-type Ca^{2+} channels during excitation and therefore increase the trigger signal for E-C coupling. Second, under voltage-clamp conditions $I_{Ca(L)}$ density was unchanged in SHR (Fig. 4), indicating unchanged L-type Ca^{2+} channel function although prolonged action potential should cause more Ca^{2+} entry during excitation. Third, under the voltage-clamp condition with unchanged trigger signal, the Ca^{2+}-induced Ca^{2+} release from the SR was significantly increased in SHR (Fig. 5), which translates to increased E-C coupling gain (Fig. 6). Prolonged action potential and increased E-C coupling gain should act synergistically to increase the Ca^{2+} transient during excitation and cause enhanced myocardial contraction (Fig. 2).

In a longitudinal view along the development of HHD, this study shows that the prehypertensive SHR (4–6 wk old) has E-C coupling parameters similar to those of age-matched WKY; however, the onset of hypertension in SHR (8–12 wk old) is associated with immediate remodeling of the E-C coupling characterized by *1*) augmented Ca^{2+} transient, *2*) unchanged resting level Ca^{2+}, *3*) unchanged $I_{Ca(L)}$ density, and *4*) unchanged SR Ca^{2+} load. These Ca^{2+} signaling characteristics are similar to those previously observed in 6-mo-old SHR after development of overt hypertrophy. (33) With more advanced hypertrophy at 10–11 mo of age, SHR hearts displayed not only increased systolic performance indicative of augmented systolic Ca^{2+} transient, but also delayed relaxation and increased diastolic stiffness suggesting altered diastolic Ca^{2+} handling (10, 16). Indeed, delayed relaxation of Ca^{2+} transient and elevated resting Ca^{2+} concentration was found in 20- to 24-mo old SHR at late-stage hypertrophy and heart failure (37). Together, the above data show that remodeling of the E-C coupling system develops gradually as HHD progresses through distinctive stages from hypertension to hypertrophy and then to heart failure. Our data establish that the augmented Ca^{2+} transient is not merely associated with hypertrophied hearts, but, in fact, precedes hypertrophy and possibly plays a role in inducing hypertrophy.

Functional changes in Ca^{2+} signaling pathways point to possible changes in the expression and modulation of Ca^{2+}-handling molecules. The present study show that in 8- to 12-wk-old SHR, $I_{Ca(L)}$ density was unchanged compared with age-matched WKY or 4- to 6-wk-old SHR, indicating maintained L-type Ca^{2+} channel expression. Maintained $I_{Ca(L)}$ was also observed at later stages of hypertrophy in SHR [i.e., 16-wk

(7), 6-mo (33), 3-mo and 18-mo (8)-old SHR] and in many other hypertrophy models in rodents and humans (30). With the trigger signal, $I_{Ca(L)}$ maintained, augmentation of the SR Ca^{2+} release could result from several possible causes: increased SR Ca^{2+} load, increased RyR2 expression level, or increased RyR2 activity by modulation. In 8- to 12-wk-old SHR, the SR load was found unchanged (Fig. 7); the RyR2 protein expression level is unlikely to change since the RyR2 protein expression level is identical in 6-mo-old SHR and WKY (33). Hence, it is most likely that augmented SR Ca^{2+} release in 8- to 12-wk-old SHR is caused by modulation of RyR2 activity at the onset of hypertension.

It has been proposed that RyR2 activity can be modulated by protein kinase A phosphorylation at the serine 2808 site (26, 27) or by Ca^{2+}/calmodulin-dependent kinase II (CaMKII) phosphorylation at the serine 2814 site (1, 38). We detected no change of RyR2 serine 2808 phosphorylation in SHR during early stages of hypertension and hypertrophy until late-stage heart failure (>1.5 yr old) (9). Since CaMKII activity was found to be elevated in 12- to 13-wk-old SHR (5), it is likely that CaMKII phosphorylation of RyR2 serine 2814 may cause increased RyR2 activity at the onset of hypertension.

In summary, the present study is the first to demonstrate in a progressive HHD model that profound changes in Ca^{2+} signaling already occur at the onset of hypertension and precede hypertrophy development. Functionally, hypertension-induced augmentation of Ca^{2+} transient causes an acute enhancement of myocardial contraction that serves to compensate, at least partially, for the increased workload to maintain the cardiac output. However, increased Ca^{2+} signaling strength should also cascade through the calmodulin, calcineurin, and CaMKII signaling pathways that are known to induce gene transcription and hypertrophic cell growth (19, 21, 28, 31, 39–41). Therefore, upregulated Ca^{2+} signaling is expected to induce cardiac hypertrophy under prolonged exposure to systemic hypertension. This immediate link between essential hypertension and upregulation of Ca^{2+} signaling provides new insights into possible therapeutic strategies for early prevention of HHD.

ACKNOWLEDGMENTS

We thank Drs. Stephen Shorofsky, Chris Ward, Yibin Wang, Bradley Nuss and George Rodney for insightful scientific discussions.

GRANTS

This work was funded by American Heart Association (AHA) National Center Scientist Development Grant 0335250N (Y. Chen-Izu), National Institutes of Health (NIH) K25 Grant HL-068704 (L. T. Izu) and NIH R01 Grant HL-071865 (C. W. Balke). S. M. Scharf was supported by AHA Grant-in-Aid 0655487U. Y. Chen-Izu was also supported by the NIH Interdisciplinary Training Program in Muscle Biology at the University of Maryland, Baltimore during the early part of this project.

REFERENCES

1. **Ai X, Curran JW, Shannon TR, Bers DM, Pogwizd SM.** Ca^{2+}/calmodulin-dependent protein kinase modulates cardiac ryanodine receptor phosphorylation and sarcoplasmic reticulum Ca^{2+} leak in heart failure. *Circ Res* 97: 1314–1322, 2005.
2. **Bailey BA, Houser SR.** Calcium transients in feline left ventricular myocytes with hypertrophy induced by slow progressive pressure overload. *J Mol Cell Cardiol* 24: 365–373, 1992.
3. **Beuckelmann DJ, Nabauer M, Erdmann E.** Intracellular calcium handling in isolated ventricular myocytes from patients with terminal heart failure. *Circulation* 85: 1046–1055, 1992.
4. **Bing OH, Brooks WW, Robinson KG, Slawsky MT, Hayes JA, Litwin SE, Sen S, Conrad CH.** The spontaneously hypertensive rat as a model of the transition from compensated left ventricular hypertrophy to failure. *J Mol Cell Cardiol* 27: 383–396, 1995.
5. **Boknik P, Heinroth-Hoffmann I, Kirchhefer U, Knapp J, Linck B, Luss H, Muller T, Schmitz W, Brodde OE, Neumann J.** Enhanced protein phosphorylation in hypertensive hypertrophy. *Cardiovasc Res* 51: 717–728, 2001.
6. **Brooks WW, Bing OH, Litwin SE, Conrad CH, Morgan JP.** Effects of treppe and calcium on intracellular calcium and function in the failing heart from the spontaneously hypertensive rat. *Hypertension* 24: 347–356, 1994.
7. **Brooksby P, Levi AJ, Jones JV.** The electrophysiological characteristics of hypertrophied ventricular myocytes from the spontaneously hypertensive rat. *J Hypertens* 11: 611–622, 1993.
8. **Cerbai E, Barbieri M, Li Q, Mugelli A.** Ionic basis of action potential prolongation of hypertrophied cardiac myocytes isolated from hypertensive rats of different ages. *Cardiovasc Res* 28: 1180–1187, 1994.
9. **Chen-Izu Y, Ward CW, Stark W Jr, Banyasz T, Sumandea MP, Balke CW, Izu LT, Wehrens XHT.** Phosphorylation of RyR2 and shortening of RyR2 cluster spacing in spontaneously hypertensive rat with heart failure. *Am J Physiol Heart Circ Physiol* (July 13, 2007). doi:10.1152/ajpheart.00562.2007.
10. **Cingolani OH, Yang XP, Cavasin MA, Carretero OA.** Increased systolic performance with diastolic dysfunction in adult spontaneously hypertensive rats. *Hypertension* 41: 249–254, 2003.
11. **Coleman TG, Guyton AC.** Hypertension caused by salt loading in the dog. 3. Onset transients of cardiac output and other circulatory variables. *Circ Res* 25: 153–160, 1969.
12. **Conrad CH, Brooks WW, Robinson KG, Bing OH.** Impaired myocardial function in spontaneously hypertensive rats with heart failure. *Am J Physiol Heart Circ Physiol* 260: H136–H145, 1991.
13. **Devereux RB, Casale PN, Hammond IW, Savage DD, Alderman MH, Campo E, Alonso DR, Laragh JH.** Echocardiographic detection of pressure-overload left ventricular hypertrophy: effect of criteria and patient population. *J Clin Hypertens* 3: 66–78, 1987.
14. **Doggrell SA, Brown L.** Rat models of hypertension, cardiac hypertrophy and failure. *Cardiovasc Res* 39: 89–105, 1998.
15. **Dorn GW II, Robbins J, Sugden PH.** Phenotyping hypertrophy: eschew obfuscation. *Circ Res* 92: 1171–1175, 2003.
16. **Engelmann GL, Vitullo JC, Gerrity RG.** Morphometric analysis of cardiac hypertrophy during development, maturation, and senescence in spontaneously hypertensive rats. *Circ Res* 60 487–494, 1987.
17. **Fields LE, Burt VL, Cutler JA, Hughes J, Roccella EJ, Sorlie P.** The burden of adult hypertension in the United States 1999 to 2000: a rising tide. *Hypertension* 44: 398–404, 2004.
18. **Gomez AM, Valdivia HH, Cheng H, Lederer MR, Santana LF, Cannell MB, McCune SA, Altschuld RA, Lederer WJ.** Defective excitation-contraction coupling in experimental cardiac hypertrophy and heart failure. *Science* 276: 800–806, 1997.
19. **Gruver CL, DeMayo F, Goldstein MA, Means AR.** Targeted developmental overexpression of calmodulin induces proliferative and hypertrophic growth of cardiomyocytes in transgenic mice. *Endocrinology* 133: 376–388, 1993.
20. **Grynkiewicz G, Poenie M, Tsien RY.** A new generation of Ca^{2+} indicators with greatly improved fluorescence properties. *J Biol Chem* 260: 3440–3450, 1985.
21. **Heineke J, Molkentin JD.** Regulation of cardiac hypertrophy by intracellular signalling pathways. *Nat Rev Mol Cell Biol* 7: 589–600, 2006.
22. **Hinderliter AL, Light KC, Willis PW.** Patients with borderline elevated blood pressure have enhanced left ventricular contractility. *Am J Hypertens* 8: 1040–1045, 1995.
23. **Janczewski AM, Lakatta EG, Stern MD.** Voltage-independent changes in L-type Ca^{2+} current uncoupled from SR Ca^{2+} release in cardiac myocytes. *Am J Physiol Heart Circ Physiol* 279: H2024–H2031, 2000.
24. **Laemmli UK.** Cleavage of structural proteins during the assembly of the head of bacteriophage T4. *Nature* 227: 680–685, 1970.
25. **Lowry DH, Rosebrough NJ, Farr AL, Randall RJ.** Protein measurement with the Folin phenol reagent. *J Biol Chem* 193: 265–275, 1951.
26. **Marks AR, Reiken S, Marx SO.** Progression of heart failure: is protein kinase A hyperphosphorylation of the ryanodine receptor a contributing factor? *Circulation* 105: 272–275, 2002.
27. **Marx SO, Reiken S, Hisamatsu Y, Jayaraman T, Burkhoff D, Rosemblit N, Marks AR.** PKA phosphorylation dissociates FKBP12.6 from the

calcium release channel (ryanodine receptor): defective regulation in failing hearts. *Cell* 101: 365–376, 2000.
28. **Molkentin JD.** Calcineurin and beyond: cardiac hypertrophic signaling. *Circ Res* 87: 731–738, 2000.
29. **Movsesian MA, Karimi M, Green K, Jones LR.** Ca^{2+}-transporting ATPase, phospholamban, and calsequestrin levels in nonfailing and failing human myocardium. *Circulation* 90: 653–657, 1994.
30. **Mukherjee R, Spinale FG.** L-type calcium channel abundance and function with cardiac hypertrophy and failure: a review. *J Mol Cell Cardiol* 30: 1899–1916, 1998.
31. **Obata K, Nagata K, Iwase M, Odashima M, Nagasaka T, Izawa H, Murohara T, Yamada Y, Yokota M.** Overexpression of calmodulin induces cardiac hypertrophy by a calcineurin-dependent pathway. *Biochem Biophys Res Commun* 338: 1299–1305, 2005.
32. **Pfeffer JM, Pfeffer MA, Fishbein MC, Frohlich ED.** Cardiac function and morphology with aging in the spontaneously hypertensive rat. *Am J Physiol Heart Circ Physiol* 237: H461–H468, 1979.
33. **Shorofsky SR, Aggarwal R, Corretti M, Baffa JM, Strum JM, Al Seikhan BA, Kobayashi YM, Jones LR, Wier WG, Balke CW.** Cellular mechanisms of altered contractility in the hypertrophied heart: big hearts, big sparks. *Circ Res* 84: 424–434, 1999.
34. **Sipido KR, Wier WG.** Flux of Ca^{2+} across the sarcoplasmic reticulum of guinea-pig cardiac cells during excitation-contraction coupling. *J Physiol* 435: 605–630, 1991.
35. **Teichholz LE, Kreulen T, Herman MV, Gorlin R.** Problems in echocardiographic volume determinations: echocardiographic-angiographic correlations in the presence of absence of asynergy. *Am J Cardiol* 37: 7–11, 1976.
36. **Vasan RS, Levy D.** The role of hypertension in the pathogenesis of heart failure. A clinical mechanistic overview. *Arch Intern Med* 156: 1789–1796, 1996.
37. **Ward ML, Pope AJ, Loiselle DS, Cannell MB.** Reduced contraction strength with increased intracellular [Ca^{2+}] in left ventricular trabeculae from failing rat hearts. *J Physiol* 546: 537–550, 2003.
38. **Wehrens XH, Lehnart SE, Reiken SR, Marks AR.** Ca^{2+}/calmodulin-dependent protein kinase II phosphorylation regulates the cardiac ryanodine receptor. *Circ Res* 94: e61–e70, 2004.
39. **Wilkins BJ, Molkentin JD.** Calcium-calcineurin signaling in the regulation of cardiac hypertrophy. *Biochem Biophys Res Commun* 322: 1178–1191, 2004.
40. **Zhang T, Brown JH.** Role of Ca^{2+}/calmodulin-dependent protein kinase II in cardiac hypertrophy and heart failure. *Cardiovasc Res* 63: 476–486, 2004.
41. **Zhang T, Johnson EN, Gu Y, Morissette MR, Sah VP, Gigena MS, Belke DD, Dillmann WH, Rogers TB, Schulman H, Ross J Jr, Brown JH.** The cardiac-specific nuclear delta B isoform of Ca^{2+}/calmodulin-dependent protein kinase II induces hypertrophy and dilated cardiomyopathy associated with increased protein phosphatase 2A activity. *J Biol Chem* 277: 1261–1267, 2002.